Reactivity of allene at phosphine-bridged di-iron centres: X-ray crystal structures of $[Fe_2(CO)_5\{\mu\text{-}\sigma,\eta^3\text{-}C(O)C(CH_2)_2\}(\mu\text{-dppm})]$ and $[Fe_2(CO)_4\{\mu\text{-}\eta^3,\eta^{3'}\text{-}(CH_2)_2C_2(CH_2)_2\}(\mu\text{-dppm})]\cdot Et_2O$

Selby A.R. Knox*, David A.V. Morton, A. Guy Orpen and Michael L. Turner
School of Chemistry, The University, Bristol BS8 1TS (UK)

(Received January 14, 1994)

Abstract

Photochemically induced reaction of $[Fe_2(CO)_6(\mu\text{-CO})(\mu\text{-dppm})]$ (**1**) (dppm = bis(diphenylphosphino)methane) with allene gave $[Fe_2(CO)_5\{\mu\text{-}\sigma,\eta^3\text{-}C(O)C(CH_2)_2\}(\mu\text{-dppm})]$ (**3**), as a result of allene–CO linking, $[Fe_2(CO)_5\{\mu\text{-}\sigma,\eta^3\text{-}C(CH_2)_2\}(\mu\text{-dppm})]$ (**4**) and $[Fe_2(CO)_4\{\mu\text{-}\eta^3,\eta^{3'}\text{-}(CH_2)_2C_2(CH_2)_2\}(\mu\text{-dppm})]$ (**5**), formed by linking of two allene molecules via the central carbons. On heating in tetrahydrofuran complex **3** decarbonylated to give **4**, which in refluxing toluene isomerised to $[Fe_2(CO)_5(PPh_2Me)(\mu\text{-}\sigma,\eta^4\text{-}CHCHCHPPh_2)]$ (**8**) and $[Fe_2(CO)_5(\mu\text{-}\eta^4\text{-}CHPhCHCHPPhMe)(\mu\text{-}PPh_2)]$ (**9**) via cleavage of a P–CH_2 bond of the dppm ligand and subsequent P–C bond formation, hydrogen shifts and, in the case of **9**, phenyl migration. Reaction of $[Fe_2(CO)_6(\mu\text{-}CH_2PPh_2)(\mu\text{-}PPh_2)]$ (**2**) with allene gave $[Fe_2(CO)_5\{\mu\text{-}PPh_2C(CH_2)_2\}(\mu\text{-}CH_2PPh_2)]$ (**10**), which contains a novel phospha-trimethylenemethane ligand produced by the insertion of allene into the phosphido bridge. Protonation of **10** in the presence of carbon monoxide gave $[Fe_2(CO)_7\{\eta^1\text{-}PPh_2C(Me)=CH_2\}(\mu\text{-}CH_2PPh_2)][BF_4]$ (**11**), containing a 2-propenylphosphine ligand. The structures of **3** and $\mathbf{5}\cdot Et_2O$ were determined by X-ray diffraction.

Key words: Crystal structures; Photochemistry; Iron complexes; Carbonyl complexes; Allene complexes; Dinuclear complexes

Introduction

In recent years we have studied the synthesis, structure and reactivity of a number of organic species, including alkyls, alkenes, alkynes and alkylidenes, at dinuclear metal centres in complexes [1]. By studying such model systems it is hoped that the construction of new homogeneous catalysts will be facilitated and that a better understanding of the chemistry which occurs on a metal surface during heterogeneous catalysis will be achieved. In this paper, we report an extension of these studies to the reaction of allene (1,2-propadiene) with the diphosphine-bridged di-iron complex $[Fe_2(CO)_6(\mu\text{-CO})(\mu\text{-dppm})]$ (**1**) [2], describing the coupling of allene with CO and with itself.

Complex **1** was chosen for investigation because previous studies of dimetallic complexes had been considerably enhanced by using the stabilising effect of bridging diphosphine ligands to suppress the dissociation of dinuclear metal complexes to mononuclear species [3]. For example, while the reaction of $[Fe_2(CO)_9]$ with ethyne had for many years been known to give the mono-iron tropone complex $[Fe(CO)_3(\eta^4\text{-}C_6H_6O)]$ [4], studies in this laboratory with **1** and ethyne showed, through the isolation and identification of intermediates, how the tropone molecule was constructed stepwise at the di-iron centre [5].

Recent studies of the thermal reactions of diphosphine-bridged di-iron complexes in this laboratory have shown that the phosphine ligand is not always an innocent spectator but can undergo a variety of transformations at high temperature [6–8]. Examples include P–C, C–C and C–H bond cleavage and formation, the rapid quantitative cleavage of the dppm ligand of complex **1** at 64 °C to give $[Fe_2(CO)_6(\mu\text{-}CH_2PPh_2)(\mu\text{-}PPh_2)]$ (**2**), containing μ-phosphido-methyl and μ-phosphido ligands, emphasising the ease with which such processes can occur [6]. These processes are now recognised to play a significant role in the deactivation of organometallic catalysts based on phosphines [9].

*Author to whom correspondence should be addressed.

SSDI 0020-1693(94)03873-M

We have shown that ethyne inserts into the Fe–CH_2 bond of the μ-phosphidomethyl group in **2** to give $[Fe_2(CO)_5(\mu\text{-}CHCHCH_2PPh_2)(\mu\text{-}PPh_2)]$, with retention of the bridging phosphido ligand [10]. The selectivity of this reaction is unusual in that earlier reports have revealed that insertion of alkynes into bridging phosphido ligands occurs readily [11–13]. In the light of the insertion of allene into a phosphido bridge of $[Mn_2(\mu\text{-}PPh_2)_2(CO)_8]$, to produce $[Mn_2\{\mu\text{-}\eta^3\text{-}PPh_2C(CH_2)_2\}(\mu\text{-}PPh_2)(CO)_7]$ [14], we also describe herein the reaction of **2** with allene and compare the selectivity with that of the reaction involving **1**. It was found that the sequence of reactions is important, since the products of the photochemical reaction of **1** with allene followed by thermolysis were very different from the products obtained by thermolysis of **1** to produce **2**, followed by the photochemical reaction of **2** with allene.

Results and discussion

Reaction of allene with $[Fe_2(CO)_6(\mu\text{-}CO)(\mu\text{-}dppm)]$ (1)

UV irradiation of a toluene solution of $[Fe_2(CO)_6(\mu\text{-}CO)(\mu\text{-}dppm)]$ (**1**) and an excess of allene for 1–3 h led to the formation of three air-stable, yellow crystalline products, isolated by column chromatography. These were identified as $[Fe_2(CO)_5\{\mu\text{-}\sigma,\eta^3\text{-}C(O)C(CH_2)_2\}(\mu\text{-}dppm)]$ (**3**), $[Fe_2(CO)_5\{\mu\text{-}\sigma,\eta^3\text{-}C(CH_2)_2\}(\mu\text{-}dppm)]$ (**4**) and $[Fe_2(CO)_4\{\mu\text{-}\eta^3,\eta^{3\prime}\text{-}(CH_2)_2C_2(CH_2)_2\}(\mu\text{-}dppm)]$ (**5**) (see Scheme 1) and characterised by a combination of analytical and spectroscopic data (Tables 1 and 2) and, for **3** and **5**, by X-ray diffraction studies.

The yields of the three products varied with the time of irradiation, as shown below, suggesting that the complexes are formed in the sequence **3** → **4** → **5**. Indeed, complex **3** is converted readily to **4** on warming (see below), in a similar decarbonylation pathway to that reported for the synthesis of $[(OC)_2Fe(\mu\text{-}dppm)\{\mu\text{-}\sigma,\eta^3\text{-}C(CH_2)_2\}Pt(PPh_3)]$ from $[(OC)_3Fe(\mu\text{-}dppm)(\mu\text{-}CO)Pt(PPh_3)]$ and allene via the allene–CO linked species $[(OC)_3Fe(\mu\text{-}dppm)\{\mu\text{-}C(O)CH_2C(=CH_2)\}Pt(PPh_3)]$ [15]. Heptacarbonyl analogues of **3** and **4** have been prepared by the photochemical reaction of iron pentacarbonyl with allene [16].

Product	Yield (%)		
	1 h	2 h	3 h
3	10	3	3
4	22	7	5
5	12	20	24

The IR spectrum of **3** showed five stretches for the terminal carbonyl ligands, as well as a low frequency band for the ketonic carbonyl ligand at 1663 cm^{-1}. The presence of this group was confirmed by a resonance at δ 225.1 (dd, J_{CP} 3, 16 Hz) in the ^{13}C NMR spectrum. The spectroscopic data did not unambiguously define

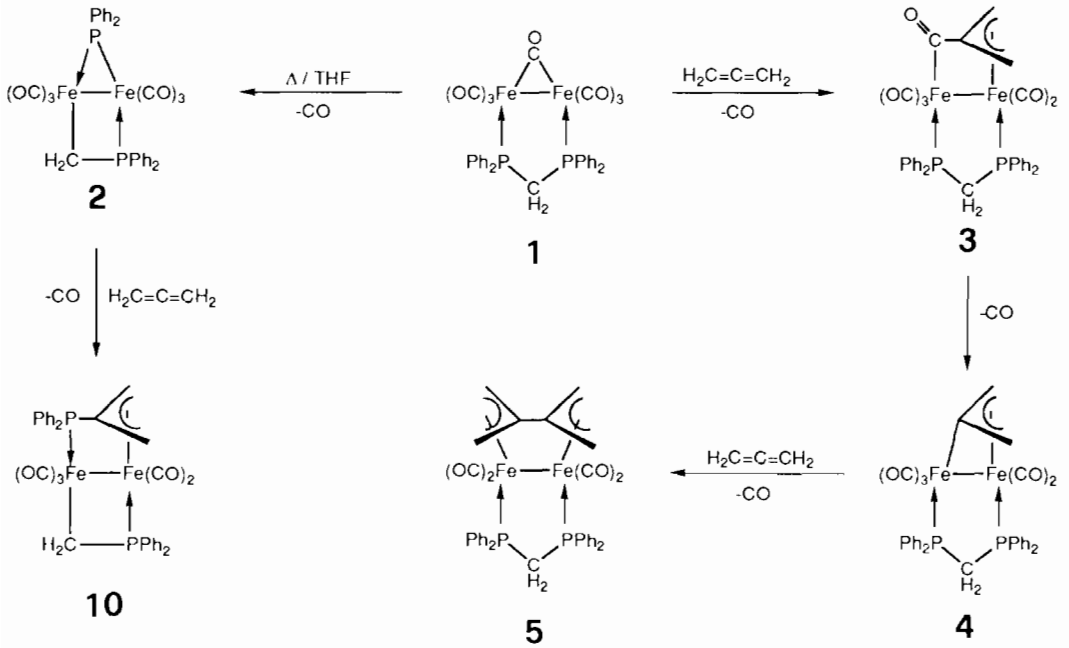

Scheme 1. Reactions of allene with $[Fe_2(CO)_6(\mu\text{-}CO)(\mu\text{-}dppm)]$ (**1**) and $[Fe_2(CO)_6(\mu\text{-}CH_2PPh_2)(\mu\text{-}PPh_2)]$ (**2**). All phenyl group hydrogens have been omitted for clarity.

TABLE 1. Analytical and other data for new complexes

Compound	Colour	$M^{a,b}$	Elemental analysis[a] (%)	
			C	H
$[Fe_2(CO)_5\{\mu\text{-}\sigma,\eta^3\text{-}C(O)C(CH_2)_2\}(\mu\text{-dppm})]$ (**3**)	yellow	676(704)[c]	57.41(57.95)	3.87(3.69)
$[Fe_2(CO)_5\{\mu\text{-}\sigma,\eta^3\text{-}C(CH_2)_2\}(\mu\text{-dppm})]$ (**4**)	yellow	676(676)	58.23(58.58)	3.95(3.85)
$[Fe_2(CO)_4\{\mu\text{-}\eta^3,\eta^{3'}\text{-}(CH_2)_2C_2(CH_2)_2\}(\mu\text{-dppm})]$ (**5**)	yellow	689(688)[d]	61.06(61.05)	4.61(4.36)
$[Fe_2(CO)_5(PPh_2Me)(\mu\text{-}\sigma,\eta^4\text{-CHCHCHPPh}_2)]$ (**8**)	red	676(676)	58.72(58.58)	4.06(3.85)
$[Fe_2(CO)_5(\mu\text{-}\eta^4\text{-CHPhCHCHPPhMe})(\mu\text{-PPh}_2)]$ (**9**)	red	676(676)	58.88(58.58)	3.93(3.85)
$[Fe_2(CO)_5\{\mu\text{-}\sigma,\eta^3\text{-}PPh_2C(CH_2)_2\}(\mu\text{-}CH_2PPh_2)]$ (**10**)	red	677(676)[d]	59.00(58.58)	4.24(3.85)
$[Fe_2(CO)_7\{\eta^1\text{-}PPh_2C(Me)=CH_2\}(\mu\text{-}CH_2PPh_2)][BF_4]$ (**11**)	red	733(733)[e]	–[f]	–[f]

[a]Calculated values in parentheses. [b]EI mass spectrometry, unless otherwise stated. [c]M − CO observed. [d]FAB mass spectrum, MH^+ observed. [e]FAB mass spectrum for cation. [f]Complex decomposed on attempted analysis.

the nature of **3** and the structure was therefore determined by X-ray crystallography.

Structure of $[Fe_2(CO)_5\{\mu\text{-}\sigma,\eta^3\text{-}C(O)C(CH_2)_2\}(\mu\text{-dppm})]$ (3)

The molecular geometry is shown in Fig. 1, with important bond lengths and angles given in Table 3. The two iron atoms are bridged by a single dppm ligand to give a five-membered ring with an Fe–Fe distance of 2.816(1) Å, consistent with the expected metal–metal single bond. This distance is *c.* 0.1 Å longer than that in $[Fe_2(CO)_6(\mu\text{-CO})(\mu\text{-dppm})]$ in which the iron–iron bond is bridged by dppm and carbonyl ligands [2].

In **3** a carbonyl ligand has linked with the central carbon of allene to produce a μ-$C(O)C(CH_2)_2$ ligand. This group is σ-coordinated to one iron and η^3-allyl coordinated to the other with Fe(1), Fe(2), C(10) and C(11) forming a virtually planar four-membered ring. The C(11)–C(12) and C(11)–C(13) distances are identical (1.404(5), 1.406(4) Å) and are typical of those observed in other η^3-allyl ligands [17]. The C(11)–C(10) bond (1.497(4) Å) is inclined at *c.* 13° to the plane of the η^3-allyl ligand. The ketonic nature of the acyl carbonyl is shown in the metal–carbon and carbon–oxygen distances, which are both significantly longer than those for the terminal carbonyl ligands in **3** (see Table 3). These acyl bond lengths are similar to the values recorded for the analogous groups in $[Fe_2(CO)_5(\mu\text{-CHCHCO})(\mu\text{-dppm})]$ [7] and $[(OC)_3Fe(\mu\text{-dppm})\{\mu\text{-}C(O)CH_2C(=CH_2)\}Pt(PPh_3)]$ [15]. In the latter complex it is the methylene group of the allene which links with the acyl carbonyl ligand. Although the linking of the central carbon of allene with a carbonyl ligand has previously been characterised spectroscopically [16, 18], complex **3** appears to be the only example of the μ-$C(O)C(CH_2)_2$ ligand to be characterised by X-ray crystallography. The FePCPFe five-membered ring in **3** is significantly twisted from the more usual envelope conformation [19], with the P–Fe–Fe–P torsion angle being 30.2(1)°. This conformation is similar to that observed in $[(OC)_2Fe(\mu\text{-dppm})\{\eta^4\text{-}(CH_2)(CMe_2)CPt(PPh_3)\}]$ [15].

The μ-σ,η^3-allene complex **4** is fluxional at room temperature, the ^1H NMR spectrum showing three broad resonances at δ 4.24, 3.39 and 2.29, each of intensity 2H. On warming, these signals sharpened and at 80 °C appeared as a triplet at δ 4.1 (J_{HP} 20 Hz), assigned to time-averaged equivalent methylene protons of the dppm ligand, and multiplets at δ 3.6 and 2.6, attributed to pairwise equivalent allyl protons, the former due to the *syn* protons and the latter to the *anti*. At −30 °C the fluxionality is frozen out, inequivalent methylene protons of the dppm ligand now being seen as multiplets at δ 4.34 and 4.10, and four inequivalent allyl protons at δ 3.32 (s), 3.14 (m), 2.47 (m) and 2.16 (s). This dynamic behaviour is attributed to the rapid 'flipping' of an FePCPFe ring which has a similar conformation to that in **3**, to produce a time-averaged plane of symmetry lying along the Fe–Fe bond, bisecting the μ-allene ligand. Interestingly, on further cooling of **4** to −70 °C, the resonances due to the methylene and several of the phenyl protons of the dppm ligand broaden, along with that of only one of the allyl protons. This cannot be explained by the fluxional process above and is probably due to a second low energy process, such as a slowing in the rotation of one of the phenyl rings of the dppm ligand.

The third product of the reaction between allene and **1** was the major species formed on prolonged photolysis (>2 h), identified as $[Fe_2(CO)_4\{\mu\text{-}\eta^3,\eta^{3'}\text{-}(CH_2)_2C_2(CH_2)_2\}(\mu\text{-dppm})]$ (**5**), formed by the linking of two molecules of allene via the central carbons. Peaks in the ^1H NMR spectrum at very similar chemical shifts, δ 1.49 (s), 1.43 (s), 1.28 (dd, *J* 2, 4 Hz) and 1.24 (s), were assigned to four pairs of equivalent allyl protons, consistent with the presence of a symmetry plane. In confirmation, the ^{13}C NMR spectrum showed only two resonances for the carbonyl ligands, at δ 225.1 (s) and 216.8 (t, *J* 7 Hz), one for the central carbons of the allyl ligands at 87.1 (s) ppm, a triplet for the

TABLE 2. Spectroscopic data for new complexes

Compound	ν(CO)[a] (cm^{-1})	^{31}P NMR[b] (ppm)	^{1}H NMR[b] (δ)	^{13}C NMR[b] (ppm)
$[Fe_2(CO)_5\{\mu\text{-}\sigma,\eta^3\text{-}C(O)C(CH_2)_2\}(\mu\text{-dppm})]$ (**3**)	2028m, 1984s, 1960m, 1946w, 1920w, 1963w	61.2 (d, *J* 90), 44.8 (d, *J* 90)[c]	7.03–6.93 (m, 20H, Ph), 4.03 (ddd, *J* 9, 11, 34, 1H, PC*H*HP), 3.91 (ddd, *J* 9, 11, 34, 1H, PCH*H*P), 2.82 (m, 1H, H^s), 2.43 (m, 1H, H^s), 1.74 (br, d, *J* 2, 1H, H^a), 1.26 (br, d, *J* 2, 1H, H^a)[d]	255.1 (dd, *J* 3, 16, C^{10}), 224.7 (d, *J* 12, CO), 216.1 (dd, *J* 5, 14, CO), 214.4 (dd, *J* 5, 13, CO), 208.7 (d, *J* 5, CO), 140.8–128.5 (m, Ph), 85.7 [dd, *J* 3, 14, *C*(CH_2)], 48.7 (dd, *J* 20, 27, PCH_2P), 46.8 (d, *J* 5, CH_2), 34.2 (d, *J* 4, CH_2)[c]
$[Fe_2(CO)_5\{\mu\text{-}\sigma,\eta^3\text{-}C(CH_2)_2\}(\mu\text{-dppm})]$ (**4**)	2031m, 1971s, 1911w[e]	60.0 (d, *J* 78), 49.4 (d, *J* 78)[f]	7.13–6.94 (m, 20H, Ph), 4.34 (m, 1H, PC*H*HP), 4.10 (m, 1H, PCH*H*P), 3.32 (s, 1H, H^s), 3.14 (m, 1H, H^s), 2.47 (m, 1H, H^a), 2.16 (s, 1H, H^a)[g]	222.2 (br, s, CO), 216.3 (br, s, CO), 214.5 (s, CO), 214.3 (s, CO), 190.7 (s, CO), 138.3 [br, m, *C*(CH_2)], 73.0 (br, s, CH_2), 65.8 (br, s, CH_2)
$[Fe_2(CO)_4\{\mu\text{-}\eta^3,\eta^{3\prime}\text{-}(CH_2)_2C_2(CH_2)_2\}(\mu\text{-dppm})]$ (**5**)	1995m, 1964s, 1940mw, 1912w	56.5 (s)[c]	8.07–7.18 (m, 20H, Ph), 4.18 (dt, *J* 11, 14, 1H, PC*H*HP), 3.66 (dt, *J* 10, 14, 1H, PCH*H*P), 1.49 (s, 1H, H^s), 1.43 (m, 1H, H^s), 1.28 (dd, *J* 2, 4, 1H, H^a), 1.24 (s, 1H, H^a)	222.5 (s, CO), 216.8 (t, *J* 7, CO), 142.2–128.4 (m, Ph), 87.1 [s, *C*(CH_2)], 52.2 (t, *J* 17, PCH_2P), 40.5 (s, CH_2), 33.6 (s, CH_2)
$[Fe_2(CO)_5(PPh_2Me)(\mu\text{-}\sigma,\eta^4\text{-}CHCHCHPPh_2)]$ (**8**)	2041s, 1981m, 1971s, 1957w, 1922w	74.8 (d, *J* 7), 58.2 (d, *J* 7)[c]	8.25 (m, 1H, H^1), 7.7–7.1 (m, 20H, Ph), 5.22 (m, 1H, H^2), 2.06 (d, *J* 10, 3H, Me), 1.70 (m, 1H, H^3)[c]	222.0 (t, *J* 12, CO), 216.9 (d, *J* 22, CO), 212.75 (s, br, 3CO), 150.2 (dd, *J* 5, 12 C^1), 101.3 (d, *J* 29, C^2), 45.1 (dd, *J* 7, 39, C^3), 14.4 (d, *J* 43, Me)[c]
$[Fe_2(CO)_5(\mu\text{-}CHPhCHCHPPhMe)(\mu\text{-}PPh_2)]$ (**9**)	2033s, 1984s, 1974m, 1948s, 1931m	166.5 (d, *J* 22), 23.0 (d, *J* 22)[c]	8.1–7.2 (m, 20H, Ph), 6.00 (dddd, *J* 1, 7, 12, 30, 1H, H^2), 4.54 (d, *J* 12, 1H, H^1), 1.98 (d, *J* 8, 1H, H^3), 0.49 (d, *J* 10, 3H, Me)[c]	218.5 (d, *J* 12, CO), 216.3 (d, *J* 12, CO), 213.9 (s, br, 3CO), 143.4–125.9 (m, Ph), 92.1 (s, C^2), 63.6 (d, *J* 8, C^1), 24.9 (d, *J* 32, C^3), 22.1 (d, *J* 23, Me)[c]
$[Fe_2(CO)_5\{\mu\text{-}\sigma,\eta^3\text{-}PPh_2C(CH_2)_2\}(\mu\text{-}CH_2PPh_2)]$ (**10**)	2038s, 1982m, 1967s, 1953w, 1923w	65.6 (d, *J* 22), 21.6 (d, *J* 20)[d]	8.18–7.07 (m, 20H, Ph), 2.15 (dd, *J* 2, 26, 1H, H^a), 1.97 (dd, *J* 2, 26, 1H, H^a), 1.72 (m, 2H, H^s), 0.74 (ddd, *J* 6, 12, 13, 1H, PC*H*H), 0.19 (dd, *J* 12, 14, 1H, PCH*H*)	223.7 (t, *J* 8, CO), 222.0 (dd, *J* 6, 14, CO), 214.8 (dd, *J* 12, 46, CO), 215.5 (dd, *J* 6, 11, CO), 210.5 (dd, *J* 5, 26, CO), 145.9–128.4 (m, Ph), 59.6 [d, *J* 43, *C*(CH_2)], 51.8 (dd, *J* 5, 14, CH_2), 39.4 (d, *J* 12, CH_2), −22.5 (dd, *J* 5, 15, PCH_2)
$[Fe_2(CO)_7\{\sigma\text{-}PPh_2CMe{=}CH_2\}(\mu\text{-}CH_2PPh_2)][BF_4]$ (**11**)	2107s, 2057m, 2043s, 2024sh, 1993w, 1961w[e]	53.2 (d, *J* 42), 29.2 (d, *J* 42)	7.70–7.60 (m, 20H, Ph), 6.29 (d, *J* 44, 1H, H^a), 6.20 (d, *J* 19, 1H, H^b), 1.73 (d, *J* 11, 3H, Me), 1.51 (d, *J* 6, 2H, PCH_2)	210.1 (br, 6CO), 200.5 (s, CO), 137.6 (d, *J* 39, $=CH_2$), 134.0–129.7 (m, Ph), 128.5 (d, *J* 46, PCMe), 22.0 (d, *J* 9, Me), −20.1 (d, *J* 14, PCH_2)

[a]Hexane solution unless otherwise stated. [b]CD_2Cl_2 solution unless otherwise stated, coupling constants (*J*) in Hz. [c]$CDCl_3$ solution. [d]Toluene-d^8 solution. [e]CH_2Cl_2 solution. [f]C_6D_6 solution. [g]Recorded at −30 °C.

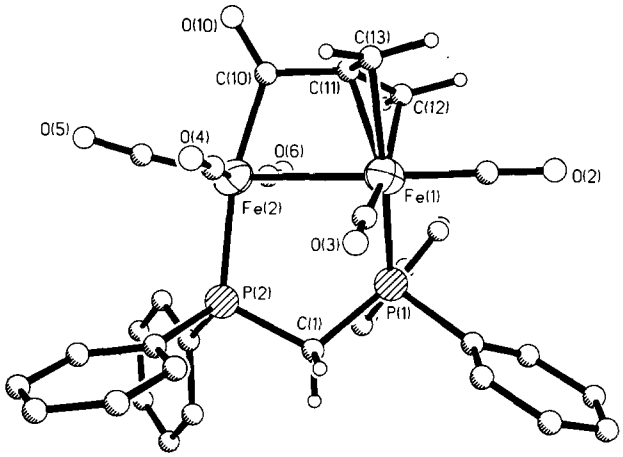

Fig. 1. Molecular structure of $[Fe_2(CO)_5\{\mu\text{-}C(O)C(CH_2)_2\}(\mu\text{-}dppm)]$ (**3**). All phenyl group hydrogens have been omitted for clarity.

methylene carbon of the dppm ligand at 52.2 ppm (J 17 Hz), and only two resonances for the terminal methylene carbons of the allyl groups at 40.5 (s) and 33.6 (s) ppm. The structure of **5** was firmly established by an X-ray diffraction study of crystals of its diethyl ether solvate.

Structure of $[Fe_2(CO)_4\{\mu\text{-}\eta^3,\eta^{3\prime}\text{-}(CH_2)_2C_2(CH_2)_2\}(\mu\text{-}dppm)]$ $(5\cdot Et_2O)$

The molecular structure of **5** is illustrated in Fig. 2, with selected bond lengths and angles given in Table 4. The molecule shows some distortion from mirror symmetry (mirror plane normal to the Fe–Fe bond) and distorted octahedral coordination around each iron atom. The geometry of the allyl groups is essentially identical to that described earlier for **3** and typical of other η^3-allyl ligands [17]. Each allyl ligand spans sites *cis* and *trans* to a phosphorus of the dppm ligand. The central C(13)–C(14) distance (1.457(13) Å) is typical of a $C_{sp^2}-C_{sp^2}$ single bond. The bis-(η^3-allyl) ligand is not planar and the two allyl planes are twisted by 25° about the central C(13)–C(14) bond. The central C–C bond is also rotated with respect to the Fe–Fe bond by 8.6°. The resultant twist of the iron coordination

TABLE 3. Selected bond lengths (Å) and angles (°) for $[Fe_2(CO)_5\{\mu\text{-}C(O)C(CH_2)_2\}(\mu\text{-}dppm)]$ (**3**)

Fe(1)–Fe(2)	2.816(1)	Fe(2)–C(10)	1.971(3)	O(6)–C(6)	1.140(3)
Fe(1)–P(1)	2.226(1)	Fe(2)–C(6)	1.796(3)	Fe(1)–C(2)	1.781(3)
P(1)–C(1)	1.842(3)	C(10)–C(11)	1.497(4)	Fe(1)–C(3)	1.765(3)
P(2)–C(1)	1.837(2)	C(11)–C(12)	1.404(5)	Fe(1)–C(11)	2.066(3)
O(2)–C(2)	1.137(4)	C(11)–C(13)	1.406(4)	Fe(1)–C(12)	2.148(3)
O(3)–C(3)	1.150(3)	Fe(1)–C(13)	2.142(3)	O(4)–C(4)	1.138(3)
Fe(2)–P(2)	2.256(1)	O(5)–C(5)	1.152(4)	Fe(2)–C(4)	1.801(3)
O(10)–C(10)	1.196(3)	Fe(2)–C(5)	1.771(3)		
Fe(2)–Fe(1)–P(1)	84.7(1)	P(2)–Fe(2)–C(6)	93.0(1)		
Fe(2)–Fe(1)–C(2)	170.8(1)	C(4)–Fe(2)–C(6)	168.0(1)		
P(1)–Fe(1)–C(2)	92.7(1)	C(5)–Fe(2)–C(6)	94.3(1)		
Fe(2)–Fe(1)–C(3)	94.8(1)	Fe(1)–Fe(2)–C(10)	73.3(1)		
P(1)–Fe(1)–C(3)	95.1(1)	P(2)–Fe(2)–C(10)	168.0(1)		
C(2)–Fe(1)–C(3)	94.3(1)	C(4)–Fe(2)–C(10)	87.5(1)		
Fe(2)–Fe(1)–C(11)	68.5(1)	C(5)–Fe(2)–C(10)	93.5(1)		
P(1)–Fe(1)–C(11)	134.4(1)	C(6)–Fe(2)–C(10)	83.8(1)		
C(2)–Fe(1)–C(11)	107.9(1)	Fe(1)–P(1)–C(1)	112.7(1)		
C(3)–Fe(1)–C(11)	122.3(1)	Fe(2)–P(2)–C(1)	111.4(1)		
Fe(2)–Fe(1)–C(12)	85.6(1)	P(1)–C(1)–P(2)	111.9(1)		
C(2)–Fe(1)–C(12)	105.8(1)	Fe(1)–C(2)–O(2)	179.0(3)		
C(2)–Fe(1)–C(12)	86.6(1)	Fe(1)–C(3)–O(3)	173.7(3)		
C(3)–Fe(1)–C(13)	159.0(1)	Fe(2)–C(4)–O(4)	173.9(2)		
C(11)–Fe(1)–C(12)	38.9(1)	Fe(2)–C(5)–O(5)	177.4(3)		
Fe(2)–Fe(1)–C(13)	90.6(1)	Fe(2)–C(6)–O(6)	173.2(2)		
P(1)–Fe(1)–C(13)	173.4(1)	Fe(2)–C(10)–O(10)	130.6(3)		
C(2)–Fe(1)–C(13)	91.2(1)	Fe(2)–C(10)–C(11)	107.8(2)		
C(3)–Fe(1)–C(13)	90.1(1)	O(10)–C(10)–C(11)	121.6(3)		
C(11)–Fe(1)–C(13)	39.0(1)	Fe(1)–C(11)–C(10)	110.0(2)		
C(12)–Fe(1)–C(13)	69.0(1)	Fe(1)–C(11)–C(12)	73.7(2)		
Fe(1)–Fe(2)–P(2)	95.2(1)	C(10)–C(11)–C(12)	119.5(3)		
Fe(1)–Fe(2)–C(4)	79.0(1)	Fe(1)–C(11)–C(13)	73.4(2)		
P(2)–Fe(2)–C(4)	93.9(1)	C(10)–C(11)–C(13)	118.8(3)		
Fe(1)–Fe(2)–C(5)	165.4(1)	C(12)–C(11)–C(13)	119.6(3)		
P(2)–Fe(2)–C(5)	98.2(1)	Fe(1)–C(12)–C(11)	67.4(2)		
C(4)–Fe(2)–C(5)	94.4(1)	Fe(1)–C(13)–C(11)	67.6(2)		
Fe(1)–Fe(2)–C(6)	90.7(1)				

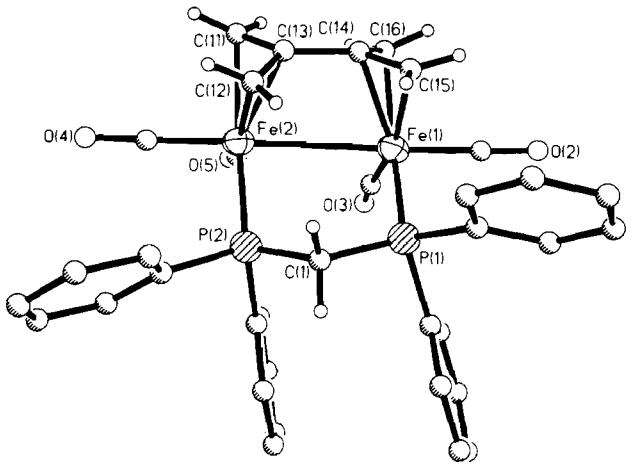

Fig. 2. Molecular structure of $[Fe_2(CO)_4\{\mu\text{-}\eta^3,\eta^{3'}\text{-}(CH_2)_2C_2(CH_2)_2\}(\mu\text{-dppm})]$ (**5**). All phenyl group hydrogens have been omitted for clarity.

spheres leads to a conformation of the dppm ligand in which the P–Fe–Fe–P torsion angle is $-15.2(1)°$ and hence there is some distortion of the Fe_2P_2C ring from the envelope conformation [19].

Two crystal structures of related bis-(η^3-allyl) complexes, $[Fe_2(CO)_6\{\mu\text{-}\eta^3,\eta^{3'}\text{-}(CH_2)_2C_2(CH_2)_2\}]$ (**6**) [20] and $[Fe_2(CO)_6\{\mu\text{-}\eta^3,\eta^{3'}\text{-}(CH_2)_4(CH)_2C_2(CH)_2(CH)_4\}]$ (**7**) [21] have been reported. The latter was produced by room temperature reaction of $[Fe_2(CO)_9]$ with 1,2-cyclononadiene and displays twisting of the central C–C bond relative to the Fe–Fe vector similar to that in **5**. The Fe–Fe distances in **5** and **7** are *c.* 3.0 Å, which is at the limit of Fe–Fe bonding interactions. An even longer distance (3.138(3) Å) was found in the non-bridged bis-(η^3-allyl) complex $[\{Fe(CO)_3(\eta^3\text{-}C_3H_5)\}_2]$ [22]. The very long Fe–Fe distances in **5** and **7** may be a consequence of the elongated 'bite' of the bisallyl ligands. This argument is the converse of that proposed to explain the reactivity of $[Pd_2(\mu\text{-}O_2CMe)_2\{\mu\text{-}\eta^3,\eta^{3'}\text{-}(CH_2)_2C_2(CH_2)_2\}]$, which readily inserts a third molecule of allene into the central C–C bond of the bis-(η^3-allyl) ligand [23]; it was proposed that the ligand is too short to bridge two Pd atoms linked by two acetate ligands (Pd–Pd *c.* 2.94 Å [24]) and therefore has to be distorted to bond effectively to each palladium. This can be discounted in the cases of **5** and **7** because the Fe–Fe bond lengths observed are very long and would certainly assume a more typical bonding distance if the ligand required it.

The solid state molecular structure of **5** differs from that suggested by the room temperature spectroscopic data, in that no symmetry plane is present. This suggests that either complex **5** adopts a different structure in solution or that it is fluxional and a process involving a rocking of the organic and dppm ligands between structures **5a** and **5b** can be proposed, as shown. This motion would create a time-averaged mirror plane perpendicular to the Fe–Fe bond in accord with the observed spectroscopic data. The process must be of low energy, since the NMR spectra of **5** are temperature independent down to -60 °C.

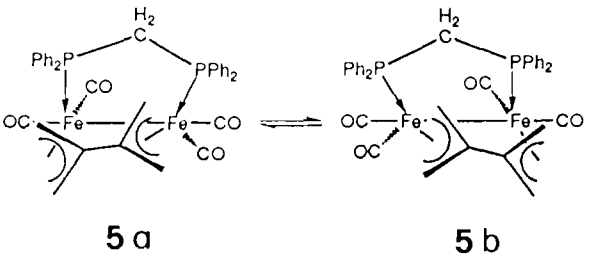

5a **5b**

Thermolysis of complexes 3, 4 and 5

Several of the dppm-bridged di-iron complexes prepared in this laboratory have proved thermally unstable, undergoing a range of P–C, C–C and C–H bond cleavage and formation processes at elevated temperatures. For example, complex **1** is rapidly transformed in solution at temperatures above 50 °C to give **2** [6], while $[Fe_2(CO)_5(\mu\text{-CHCHCO})(\mu\text{-dppm})]$, derived from the reaction of **1** with ethyne, undergoes a remarkable sequence of transformations on heating in toluene to give $[Fe_2(CO)_6\{\mu\text{-C}(CH_2Ph)PPh_2CH_2PPh\}]$ [7]. In the light of these findings, and in order to establish the likely intermediacy of **3** in the formation of **4**, the thermolysis of the di-iron allene complexes **3**, **4** and **5** was studied.

As expected, upon heating **3** under the mild conditions of refluxing tetrahydrofuran (64 °C) the allene–CO link was broken and decarbonylation occurred to give **4** rapidly and quantitatively. Interestingly, however, the reverse reaction does not occur even under 100 atm of CO at 100 °C.

In contrast to **3**, the bis-allyl complex **5** is thermally robust and is recovered unchanged from refluxing toluene (111 °C). Complex **4** shows intermediate thermal stability, undergoing isomerisation at toluene reflux to give $[Fe_2(CO)_5(PPh_2Me)(\mu\text{-}\sigma,\eta^4\text{-CHCHCHPPh}_2)]$ (**8**) and $[Fe_2(CO)_5(\mu\text{-}\eta^4\text{-CHPhCHCHPPhMe})(\mu\text{-PPh}_2)]$ (**9**). These products were formed in a combined yield of 78% but extensive chromatography was required to separate them, resulting in their isolation in yields of only 22 and 16%, respectively. Spectroscopic data identified **8** and **9** as resulting from the cleavage of $Ph_2P\text{–}CH_2$ bonds of dppm, linking of phosphorus-containing fragments with the allene, and associated hydrogen and phenyl shifts.

TABLE 4. Selected bond lengths (Å) and angles (°) for $[Fe_2(CO)_4\{\mu\text{-}\eta^3,\eta^{3\prime}\text{-}(CH_2)_2C_2(CH_2)_2\}(\mu\text{-dppm})]$ ($5\cdot Et_2O$)

Fe(1)–Fe(2)	2.992(2)	Fe(2)–C(5)	1.751(10)	O(5)–C(5)	1.159(12)
Fe(1)–P(1)	2.221(3)	Fe(2)–C(11)	2.121(10)	C(11)–C(13)	1.405(13)
Fe(1)–C(2)	1.744(10)	Fe(2)–C(12)	2.095(11)	C(12)–C(13)	1.386(14)
Fe(1)–C(3)	1.767(9)	Fe(2)–C(13)	2.037(8)	C(13)–C(14)	1.457(13)
Fe(1)–C(14)	2.034(8)	P(1)–C(1)	1.831(8)	C(14)–C(15)	1.390(13)
Fe(1)–C(15)	2.126(9)	P(2)–C(1)	1.833(7)	C(14)–C(16)	1.403(13)
Fe(1)–C(16)	2.093(9)	O(2)–C(2)	1.154(12)		
Fe(2)–P(2)	2.212(3)	O(3)–C(3)	1.142(10)		
Fe(2)–C(4)	1.749(9)	O(4)–C(4)	1.146(11)		
Fe(2)–Fe(1)–P(1)	92.9(1)	C(5)–Fe(2)–C(11)	90.4(4)		
Fe(2)–Fe(1)–C(2)	174.6(3)	Fe(1)–Fe(2)–C(12)	85.1(2)		
P(1)–Fe(1)–C(2)	91.6(3)	P(2)–Fe(2)–C(12)	95.4(2)		
Fe(2)–Fe(1)–C(3)	81.5(3)	C(4)–Fe(2)–C(12)	92.2(3)		
P(1)–Fe(1)–C(3)	105.8(3)	C(5)–Fe(2)–C(12)	157.1(4)		
C(2)–Fe(1)–C(3)	94.4(4)	C(11)–Fe(2)–C(12)	67.7(3)		
Fe(2)–Fe(1)–C(14)	67.4(3)	Fe(1)–Fe(2)–C(13)	67.8(2)		
P(1)–Fe(1)–C(14)	122.0(3)	P(2)–Fe(2)–C(13)	125.8(2)		
C(2)–Fe(1)–C(14)	112.5(4)	C(4)–Fe(2)–C(13)	111.9(4)		
C(3)–Fe(1)–C(14)	122.7(4)	C(5)–Fe(2)–C(13)	118.7(4)		
Fe(2)–Fe(1)–C(15)	92.3(1)	C(11)–Fe(2)–C(13)	39.4(3)		
P(1)–Fe(1)–C(15)	92.8(2)	Fe(1)–P(1)–C(1)	39.1(3)		
C(2)–Fe(1)–C(15)	90.5(3)	Fe(2)–P(2)–C(1)	114.8(3)		
C(3)–Fe(1)–C(15)	160.6(3)	P(1)–C(1)–P(2)	107.6(6)		
C(14)–Fe(1)–C(15)	39.0(3)	Fe(1)–C(2)–O(2)	178.3(8)		
Fe(2)–Fe(1)–C(16)	85.2(2)	Fe(1)–C(3)–O(3)	171.0(7)		
P(1)–Fe(1)–C(16)	160.4(2)	Fe(2)–C(4)–O(4)	178.2(7)		
C(2)–Fe(1)–C(16)	91.6(3)	Fe(2)–C(5)–O(5)	171.0(7)		
C(3)–Fe(1)–C(16)	93.2(3)	Fe(2)–C(11)–C(13)	67.1(4)		
C(14)–Fe(1)–C(16)	39.7(3)	Fe(2)–C(12)–C(13)	68.1(5)		
C(15)–Fe(1)–C(16)	67.8(2)	Fe(2)–C(13)–C(11)	73.5(5)		
Fe(1)–Fe(2)–P(2)	84.6(1)	Fe(2)–C(13)–C(12)	72.7(5)		
Fe(1)–Fe(2)–C(4)	175.8(3)	C(11)–C(13)–C(12)	114.6(7)		
P(2)–Fe(2)–C(4)	92.4(3)	Fe(2)–C(13)–C(14)	111.2(5)		
Fe(1)–Fe(2)–C(5)	89.8(3)	C(11)–C(13)–C(14)	120.5(7)		
P(2)–Fe(2)–C(5)	106.3(3)	C(12)–C(13)–C(14)	123.5(8)		
C(4)–Fe(2)–C(5)	93.9(4)	Fe(1)–C(14)–C(13)	12.1(6)		
Fe(1)–Fe(2)–C(11)	93.1(2)	Fe(1)–C(14)–C(15)	74.1(5)		
P(2)–Fe(2)–C(11)	163.1(2)	C(13)–C(14)–C(15)	119.9(7)		
C(4)–Fe(2)–C(11)	88.8(3)	Fe(1)–C(14)–C(16)	72.4(5)		
C(5)–Fe(2)–C(11)	90.4(4)	C(13)–C(14)–C(16)	124.0(7)		
Fe(1)–Fe(2)–C(12)	85.1(2)	C(15)–C(14)–C(16)	114.9(7)		
P(2)–Fe(2)–C(11)	163.1(2)	Fe(1)–C(15)–C(14)	66.9(4)		
C(4)–Fe(2)–C(11)	88.8(3)	Fe(1)–C(16)–C(14)	67.9(4)		

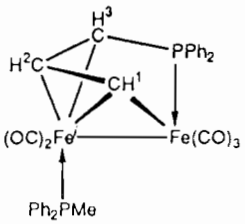

8

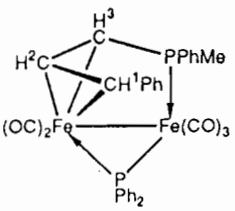

9

Complex **8** was clearly identified as an isomer of **4** by mass spectrometry, a peak for the molecular ion being associated with peaks for the loss of five carbonyl ligands. In the ^1H NMR spectrum an unresolved multiplet at δ 8.25 was assigned to the μ-alkylidene proton (H^1), which agrees well with the value of δ 8.63 for the similar proton in $[Fe_2(CO)_5(\mu\text{-CHCHCO})(\mu\text{-dppm})]$ [7]. Protons H^2 and H^3 were observed as complex multiplets at δ 5.22 and 1.70, respectively, the latter assigned, by virtue of its high field chemical shift, as being adjacent to the PPh_2 moiety. Most informative, however, the methyl group of a PPh_2Me ligand was observed as a doublet at δ 2.06 with a typical coupling of 10 Hz to phosphorus.

The ^{31}P NMR spectrum of **8** showed two doublets at δ 74.8 and 58.2 ppm (J_{PP} 7 Hz), the small size of the coupling clearly indicating that the dppm ligand was no longer intact. The doublet at δ 74.8 was assigned to the PPh_2 moiety, as part of a phosphine unit, and that at δ 58.2 to the PPh_2Me ligand. These assignments

were confirmed by the recording of a ^{31}P NMR spectrum whilst selectively decoupling the *ortho* protons of the phenyl rings. The doublet at δ 58.2 collapsed to a broad singlet whose intensity was about half that of the resonance at δ 74.8. Although the size of the $^{2}J_{PH}$ coupling was not resolved, the reduction in intensity shows that the signal at δ 58.2 can be assigned to the PPh_2Me ligand.

The proposed structure was confirmed by the ^{13}C NMR spectrum, which showed resonances at δ 14.42 (d, J 43 Hz) for the methyl group, 45.05 (dd, J 7, 39 Hz) for the carbon (C^3) directly attached to the PPh_2 group, 101.29 (d, J 29 Hz) for the central carbon (C^2) and 150.24 (dd, J 5, 12 Hz) ppm for the alkylidene carbon (C^1), assigned from their chemical shifts and the magnitude of the P–C coupling constants. Three carbonyl resonances were observed at δ 222.0 (t, J 12 Hz), 216.93 (d, J 22 Hz) and 212.75 (br, s) ppm, the broadness of the last resonance being probably due to localised carbonyl scrambling via a trigonal twist [25].

Complex **9** was also shown to be an isomer of **4**, and therefore of **8**, by virtue of its mass spectrum, which exhibited a molecular ion at 676 followed by ions due to sequential loss of five carbonyl ligands. The presence of a phosphido bridge was clearly indicated by a resonance at δ 166.5 (d, J 22 Hz) in the ^{31}P NMR spectrum. This was accompanied by a doublet at δ 23.04 (J 22 Hz) for the PPhMe moiety, the small size of the P–P coupling constant again indicating that the dppm ligand was no longer intact. The same selective decoupling experiment as described for **8** was performed and a reduction in the relative intensity of the signal at δ 23.04 observed, confirming that this resonance can be assigned to the PPhMe group.

The ^{1}H NMR spectrum of **9** was most informative, with a multiplet at δ 6.00 (dddd, J 1, 7, 12, 30 Hz) being assigned to H^2. The benzylic proton (H^1) appeared as a doublet at δ 4.54 (J 12 Hz) and was shown to be coupled to H^2 by a homonuclear decoupling experiment. A similar experiment established that a triplet resonance at δ 1.98 (J 8 Hz), assigned to H^3, was also coupled to H^2, the triplet structure suggesting a second, identical coupling to a phosphorus atom. The methyl group of the PPhMe unit was observed as a doublet at δ 0.49 (J 10 Hz), shifted to higher field compared to the methyl group of **8**, probably as a result of the reduction in the number of phenyl groups attached to the phosphorus atom. In the ^{13}C NMR spectrum the terminal carbonyl region was very similar to that of **8** with three resonances at δ 218.5 (d, J 12 Hz), 216.3 (d, J 12 Hz), and 213.9 (s, br) ppm, the broadness of the last resonance again indicating localised carbonyl scrambling in an $Fe(CO)_3$ group [25]. Further signals were observed at δ 92.1 (s) for the central carbon C^2, 63.6 (d, J 8 Hz) for the benzylic carbon C^1, 24.9 (d, J 32 Hz) for carbon C^3, and 22.1 (d, J 23 Hz) ppm for the methyl carbon of the PPhMe group. The large P–C coupling constants of the last two resonances reveal that they are both directly bound to a phosphorus atom.

Several complexes have been previously reported in which there are organic fragments structurally related to those of **8** and **9**. These were generally prepared by the linking of alkynes with bridging phosphido ligands, or phosphines with bridging alkynes [11–13, 26, 27].

The formation of **8** and **9** by the thermolysis of **4** requires a substantial number of rearrangements to take place, including P–C bond cleavage and formation, several hydrogen shifts and, in the case of **9**, a phenyl shift. No intermediate species could be detected by IR monitoring of the reaction, even at very short reaction time, and it is therefore difficult to reach firm mechanistic conclusions. It is clear, however, that since upon heating in toluene neither **8** nor **9** is converted to the other they must be formed by independent pathways. The evolution of **8** is the more easy to envisage, requiring:

(a) cleavage of dppm to give CH_2PPh_2 and PPh_2 ligands, as in the formation of **2** from **1**,

(b) oxidative addition of a C–H bond of allene, to give allyl and metal-bound hydrogen,

(c) reductive-elimination of the hydrogen with the CH_2PPh_2 group to afford Ph_2PMe,

(d) C–P bond formation involving the PPh_2 group and the allyl fragment,

(e) a hydrogen transfer to the central carbon of the allyl.

For **9** there is an additional phenyl shift, introducing even greater complexity, and the sequence of events for both is unknown.

Previous studies have shown that the thermolysis of μ-allene complexes such as $[Fe_2(CO)_7(\mu\text{-}\sigma,\eta^3\text{-}C_3H_4)]$ and $[Os_3(CO)_{11}(\mu\text{-}\sigma,\eta^3\text{-}C_3H_4)]$ does involve a hydrogen shift via the metal atom [16, 28], as suggested for the transformation of the dppm ligand in **4** to PPh_2Me. Similar conversions of dppm to PPh_2Me have been observed previously [29–31]. Phenyl migrations, such as that required to produce **9**, have also been seen in di-iron dppm chemistry, e.g. the formation of $[Fe_2(CO)_6\{\mu\text{-}C(CH_2Ph)PPh_2CH_2PPh\}]$ by the thermolysis of $[Fe_2(CO)_5(\mu\text{-}CHCHCO)(\mu\text{-dppm})]$ [7].

Reaction of $[Fe_2(CO)_6(\mu\text{-}CH_2PPh_2)(\mu\text{-}PPh_2)]$ (2) with allene

The probability that the complexes **8** and **9** arose from **4** via the cleavage of dppm to give CH_2PPh_2 and PPh_2 ligands, led naturally to a study of the reaction of complex **2** with allene. The reaction of **2** with allene could follow a number of routes, depending on whether allene insertion takes place into the $Fe\text{–}CH_2PPh_2$ bond, as for the reaction of ethyne with **2** [10], or into a metal–carbonyl bond, as for the reaction of allene with

complex **1**. In the event, a different mode of reaction for **2** was observed, as shown in Scheme 1.

A toluene solution of **2** was subjected to UV irradiation for 3 h in the presence of a large excess of allene, affording dark red crystalline $[Fe_2(CO)_5\{\mu\text{-}PPh_2C(CH_2)_2\}(\mu\text{-}CH_2PPh_2)]$ (**10**), in 50% yield. The loss of one CO and incorporation of allene was confirmed by elemental analysis and FAB mass spectrometry, the latter showing a heaviest ion at *m/z* 677, corresponding to $(M+H)^+$ and sequential loss of five carbonyl ligands. In the ^{31}P NMR spectrum two doublets were observed at δ 65.63 (J 22) and 21.64 (J 22 Hz), values which may be compared with those for the μ-PPh_2 and μ-CH_2PPh_2 ligands of **2** at δ 181.1 and 21.27, respectively. These data clearly indicated that the μ-CH_2PPh_2 ligand remained intact in the product **10** and that allene had inserted into the phosphido bridge.

The ^1H NMR spectrum of **10** confirms the regiochemistry of the reaction. The methylene protons of the μ-CH_2PPh_2 ligand appear at δ 0.74 (ddd, J 6, 12, 13) and 0.19 (dd, J 12, 14 Hz), values which agree well with those for the same ligand in **2** at δ 0.70 and 0.61. The allyl protons are observed at δ 2.15 (dd, J 2, 26), 1.97 (dd, J 2, 26 Hz) and 1.72 (m). The two signals at lower field are assigned to the *anti* protons on the basis of their large coupling to phosphorus (26 Hz) and the multiplet at δ 1.72, integrating to two protons, to the *syn* protons.

Unfortunately, crystals of **10** proved unsuitable for X-ray diffraction as they decomposed rapidly in the X-ray beam. However, the ^{13}C NMR spectrum is most informative, enabling the geometry around the iron atoms to be determined; the two phosphorus-containing bridges appear to lie *cis* to one another, as they do in the precursor **2**, with a carbonyl ligand *trans* to the phosphorus of the μ-$PPh_2C(CH_2)_2$ ligand. Resonances for the carbonyl ligands are observed at δ 223.7 (t, J 8), 222.0 (dd, J 6, 14), 215.5 (dd, J 6, 11), 214.8 (dd, J 12, 46) and 210.5 (dd, J 5, 26 Hz), the large coupling (46 Hz) of the resonance at δ 214.8 indicating that this carbonyl ligand is coordinated *trans* to the phosphorus of the μ-$PPh_2C(CH_2)_2$ ligand. A doublet of doublets at δ −22.5 (J 5, 15 Hz) ppm is due to the methylene carbon of the μ-CH_2PPh_2 ligand, the presence of two small coupling constants showing that the methylene carbon is *cis* to the phosphorus of the μ-$PPh_2C(CH_2)_2$ ligand. The chemical shift is very similar to that observed for the methylene carbon in **2** at $-\delta$ 19.5. Resonances for the allene carbons were observed at δ 59.6 (d, J 43), 51.8 (dd, J 5, 14) and 39.4 (d, J 12 Hz) ppm for the central and terminal carbons, respectively. The signal for the central carbon is moved to higher field compared with those reported earlier for **3** and **4**, as a result of its linking with phosphorus. The only other example of this type of coupling was reported recently by Mays and co-workers, who reacted $[Mn_2(\mu\text{-}PPh_2)_2(CO)_8]$ with allene and obtained $[Mn_2\{\mu\text{-}PPh_2C(CH_2)_2\}(\mu\text{-}PPh_2)(CO)_7]$ in 5% yield [14].

Protonation of $[Fe_2(CO)_5\{\mu\text{-}PPh_2C(CH_2)_2\}(\mu\text{-}CH_2PPh_2)]$ (10) in the presence of carbon monoxide

The protonation of the complexes **3, 4, 5** and **10** was investigated, but only the last gave stable, identifiable products.

Addition of a ten-fold excess of $HBF_4\cdot OEt_2$ to a dichloromethane solution of **10** while purging with CO resulted in quantitative conversion to the 2-propenylphosphine complex $[Fe_2(CO)_7\{PPh_2C(Me)=CH_2\}(\mu\text{-}CH_2PPh_2)][BF_4]$ (**11**). Complex **11** decomposed slowly as a solid but rapidly in solution to give an insoluble white solid.

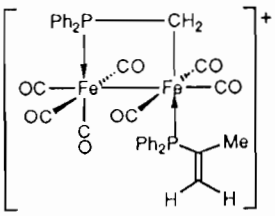

11

Six terminal carbonyl bands were observed in the IR spectrum of **11**, with the high frequencies indicative of a cation. The FAB mass spectrum showed a molecular ion for the cation at *m/z* 733 and intense peaks corresponding to the loss of three, four, six and seven carbonyl ligands. The ^1H NMR spectrum exhibited doublets at δ 6.29 (J_{HP} 44) and 6.20 (J_{HP} 19 Hz) for the propenyl methylene protons δ 1.73 (J_{HP} 11 Hz) for the methyl group of the alkenyl ligand and δ 1.51 (J_{HP} 6 Hz) for the equivalent methylene protons of the μ-CH_2PPh_2 ligand. The configuration of the ligand was confirmed by comparing the P–H couplings with those of free 1- and 2-propenylphosphine ligands [32], as shown below, while the low field chemical shifts of the propenyl methylene protons indicate that the C=C double bond is not coordinated to an iron atom. The coupling constants also agree well with those reported for $[(\eta\text{-}C_5H_5)(OC)_2Mo(\mu\text{-}H)(\mu\text{-}PPh_2)Mn(CO)_3(PPh_2PCH=CH_2)]$ [33], $[(\eta\text{-}C_5H_5)(OC)_2Mo(\mu\text{-}H)(\mu\text{-}PPh_2)Mn(CO)_3\{PPh_2PC(Me)=C(H)Me\}]$[33]and$[Mn_2(CO)_9(PPh_2CH=CH_2)]$ [34].

	Coupling constants (Hz) [32]		
	J (PMe)	J (PH^a)	J (PH^b)
$Ph_2PC(Me)=CH^a(trans)H^b(cis)$	9.2	25.3	10.7
E-$Ph_2PCH^a=CH^bMe$	0.3	7.0	10.0
Z-$Ph_2PCH^a=CH^bMe$	0	2.7	20.0

In the ^{13}C NMR spectrum, doublets at δ 137.6 (J 39) and 128.5 (J 46 Hz) were assigned to the alkenyl CH_2 and C(Me) carbons, respectively, from the size of the P–C coupling constant and by comparison with the values of δ 145.2 and 119.2 reported for $[Ph_3PCH{=}CH_2][Br]$ [35]. A doublet at δ 22.0 (J 9) was assigned to the methyl group of the phosphine ligand and one at δ −20.1 (J 14 Hz) to the methylene carbon of the μ-CH_2PPh_2 ligand. The carbonyl ligands were observed as a singlet at δ 200.5 and a broad resonance centred at δ 210, indicating the existence of a fluxional process at room temperature. Unfortunately, the low solubility of **11** prevented the recording of a low temperature ^{13}C NMR spectrum but the ^1H NMR spectrum proved to be independent of temperature down to −40 °C. The existence of the fluxional process provides strong evidence, however, that the structure of **11** is that shown, with the phosphine ligand adopting a position *cis* to the metal–metal bond and *trans* to the CH_2PPh_2 group. This has six carbonyls lying in a plane perpendicular to the μ-CH_2PPh_2 ligand, capable of undergoing a 'merry-go-round' exchange [36, 37], and one unique CO, consistent with the ^{13}C NMR spectrum observed at room temperature. The alternative structure for **11**, with the phosphine in a position *trans* to the metal–metal bond, would not permit such an exchange.

The initial step in the formation of **11** is likely to be protonation at a terminal carbon of the η^3-allyl unit in **10** to give $[Fe_2(CO)_5\{\mu\text{-}Ph_2PC(Me){=}CH_2\}(\mu\text{-}CH_2PPh_2)]^+$, in which the propenylphosphine bridges the iron–iron bond via phosphorus coordination to one metal and alkene coordination to the other. One iron atom in this species will have a 16-electron configuration, inducing the uptake of a CO, followed by a second CO displacing the double bond of the phosphine from coordination to give the observed product. Such a transformation has been seen in the conversion of $[Mn_2(CO)_8(\mu\text{-}\eta^2\text{-}PPh_2CH{=}CH_2)]$ to $[Mn_2(CO)_9(\eta^1\text{-}PPh_2CH{=}CH_2)]$ [34].

Conclusions

The reaction of $[Fe_2(CO)_6(\mu\text{-}CO)(\mu\text{-dppm})]$ (**1**) with allene under UV irradiation proceeds initially in a very similar manner to that with ethyne [5], in that in each case a product of the type $[Fe_2(CO)_5(L\text{-}CO)(\mu\text{-dppm})]$ (L = ethyne or allene) is formed resulting from linking of the hydrocarbon with carbon monoxide. With ethyne the reaction continues by insertion of a second and third alkyne molecule, followed by ring closure to afford a di-iron tropone complex. For allene, however, the initial complex **3** undergoes ready decarbonylation to give a μ-σ,η^3-allene complex **4** which appears to react with a second molecule of allene to yield a μ-$\eta^3,\eta^{3\prime}$-$(CH_2)_2C_2(CH_2)_2$ species **5** derived by linking of two allenes via their central carbon atoms.

Thermolysis of the μ-σ,η^3-allene complex **4** results in cleavage of the dppm ligand and linking of phosphorus-containing fragments with the terminal carbons of coordinated allene. However, when the dppm ligand in **1** is first cleaved, to give **2**, and this species is then treated with allene, a different product **10** is obtained, resulting from allene insertion into a μ-PPh_2 ligand via the central carbon of the hydrocarbon. This contrasts with the reaction of ethyne with **2**, when insertion into the iron–carbon bond of the μ-CH_2PPh_2 ligand was observed [10], further emphasising the delicate balance which characterises the reactions of hydrocarbons at the dppm-bridged di-iron centre.

Experimental

Reactions and general manipulations were performed under a nitrogen atmosphere using degassed solvents, dried by distillation over an appropriate drying agent. Photolysis reactions were carried out in magnetically stirred silica glass tubes held *c.* 20 cm away from a 500 W mercury vapour lamp. Separation of the reaction products was generally achieved by column chromatography on alumina, except where stated otherwise. Further purification was by crystallisation by diffusion between dichloromethane and hexane layers. Elemental analyses were performed by the Microanalytical Laboratory of the School of Chemistry, University of Bristol. Solution IR spectra were recorded on Nicolet 5-MX or Perkin-Elmer 1710 Fourier transform spectrometers, using calcium fluoride cells of 1 mm path lengths. Low resolution electron impact mass spectra were recorded using a Kratos MS-9 instrument updated with VG 2AB electronics and ion source operating at 70 eV. FAB mass spectra were provided by the SERC Mass Spectrometry Centre, Swansea. Proton and ^{13}C NMR spectra were recorded on Jeol FX 90, GX 270 and GX 400 NMR spectrometers, ^{31}P NMR spectra on Jeol FX 90 and GX 400 instruments. The complexes $[Fe_2(CO)_6(\mu\text{-}CO)(\mu\text{-dppm})]$ and $[Fe_2(CO)_6(\mu\text{-}CH_2PPh_2)(\mu\text{-}PPh_2)]$ were prepared by literature methods [2, 6].

Reaction of $[Fe_2(CO)_6(\mu\text{-}CO)(\mu\text{-dppm})]$ (1) with allene

A toluene solution (75 cm^3) of **1** (0.25 g, 0.36 mmol) was cooled in a silica Young's tube (*c.* 150 cm^3) to −196 °C and evacuated, then allene (0.43 g, 11 mmol) was condensed in. The tube was slowly warmed to room temperature and subjected to UV irradiation. Chromatography led to the isolation of three complexes in yields dependent upon the time of irradiation as de-

scribed in the text. Elution with dichloromethane–hexane (1:9) gave two orange bands, identified as $[Fe_2(CO)_5\{\mu\text{-}\sigma,\eta^3\text{-}C(CH_2)_2\}(\mu\text{-dppm})]$ (**4**) and $[Fe_2(CO)_4\{\mu\text{-}\eta^3,\eta^{3\prime}\text{-}(CH_2)_2C_2(CH_2)_2\}(\mu\text{-dppm})]$ (**5**), which each afforded dark red crystals from dichloromethane–hexane. A yellow band eluted with dichloromethane–hexane (1:1) afforded orange crystalline $[Fe_2(CO)_5\{\mu\text{-}C(O)C(CH_2)_2\}(\mu\text{-dppm})]$ (**3**).

Decarbonylation of $[Fe_2(CO)_5\{\mu\text{-}\sigma,\eta^3\text{-}C(O)C(CH_2)_2\}(\mu\text{-dppm})]$ (3)

Heating a tetrahydrofuran solution (50 cm^3) of **3** (0.11 g, 0.16 mmol) at reflux for 3 h resulted in a slight lightening of the solution and the disappearance of the carbonyl absorption at 1645 cm^{-1} in the IR spectrum. Chromatography, eluting with dichloromethane–hexane (1:9), gave a yellow band which produced a quantitative yield (0.10 g) of $[Fe_2(CO)_5\{\mu\text{-}\sigma,\eta^3\text{-}C(CH_2)_2\}(\mu\text{-dppm})]$ (**4**).

Attempted carbonylation of $[Fe_2(CO)_5\{\mu\text{-}\sigma,\eta^3\text{-}C(CH_2)_2\}(\mu\text{-dppm})]$ (4)

A toluene solution (20 cm^3) of complex **4** (50 mg, 0.07 mmol) was placed in an autoclave, and heated to 50 °C under 100 atm of CO for 10 h. No reaction was observed by IR spectroscopy. Removal of the solvent followed by chromatography developed one yellow band which provided only starting material **4** (35 mg, 70%).

Thermolysis of $[Fe_2(CO)_5\{\mu\text{-}\sigma,\eta^3\text{-}C(CH_2)_2\}(\mu\text{-dppm})]$ (4)

A toluene solution (100 cm^3) of **4** (90 mg, 0.13 mmol) was refluxed for 20 min, resulting in a colour change from orange to brown. After evaporation, the residue was extracted with hexane (30 cm^3) and subjected to chromatography. Elution with diethyl ether–hexane (1:9) produced a brown band which afforded trace amounts of an unidentified brown solid (ν(CO) (in hexane) 2019s, 1963m, 1953s cm^{-1}; ^{31}P NMR (in $CDCl_3$) δ 174.7 ppm). An orange band, eluting with diethyl

TABLE 5. Details of structure analyses

	3	**5**·Et_2O
Crystal data[a]		
Formula	$C_{34}H_{26}O_6P_2Fe_2$	$C_{39}H_{40}O_5P_2Fe_2$
M	692.2	762.4
Crystal system	monoclinic	monoclinic
Space group (No.)	$P2_1/c$ (No. 14)	$P2_1/c$ (No. 14)
a (Å)	13.777(6)	12.359(5)
b (Å)	15.019(5)	12.204(5)
c (Å)	16.221(5)	23.940(9)
β (°)	109.05(3)	93.83(3)
U (Å^3)	3172.5(21)	3602.6(25)
Z	4	4
D_c (g cm^{-3})	1.47	1.41
F(000)	1432	1584
μ(Mo Kα (cm^{-1}))	10.6	9.3
Data collection and reduction		
Crystal dimensions (mm)	0.3×0.3×0.6	0.2×0.25×0.6
2θ Range (°)	4–50	4–50
Scan method	$\omega/2\theta$	Wyckoff ω
Scan width (ω°)	$1.0+\Delta_{\alpha1\alpha2}$	1.2
Total data	6494	7300
'Observed' unique data (*NO*)	4851	3110
Observation criterion ($F_o^2 > n\sigma(F_o^2)$)	1.5	2
Transmission coefficient: min., max.	0.788, 0.929	0.587, 0.651
R_{merg}	0.029	0.012
Refinement		
Disordered atoms	none	solvent, restraints applied
Least-squares variables (*NV*)	421	491
R[b]	0.038	0.074
R_w[c]	0.039	0.059
S[d]	1.39	1.38
g	0.0007	0.0004
Final difference map features (e Å^{-3})	+0.5, −0.3	+0.7, −0.7

[a]Data common to all: $T=295$ K; wavelength 0.71073 Å. [b]$R=\Sigma|\Delta|/\Sigma|F_o|$. [c]$R_w=[\Sigma w^{1/2}|\Delta|/\Sigma w^{1/2}F_o]$. [d]$S=[\Sigma w\Delta^2/(NO-NV)]^{1/2}$. $\Delta=F_o-F_c$; $w=[\sigma_c^2(F_o)+gF_o^2]^{-1}$, $\sigma_c^2(F_o)$ = variance in F_o due to counting statistics.

ether–hexane (1:6) provided 70 mg (78%) of a mixture of $[Fe_2(CO)_5(PPh_2Me)(\mu\text{-}\eta^1,\eta^4\text{-}CHCHCHPPh_2)]$ (**8**) and $[Fe_2(CO)_5(\mu\text{-}\eta^4\text{-}PPhMeCHCHCHPh)(\mu\text{-}PPh_2)]$ (**9**) as a red solid. Partial separation of the two isomers was achieved by repeated chromatography, eluting with diethyl ether–hexane (1:9), to give 20 mg (22%) of **8**, 35 mg of a mixture and 15 mg (16%) of **9**.

Thermolysis of $[Fe_2(CO)_5(PPh_2Me)(\mu\text{-}\eta^1,\eta^4\text{-}CHCHCHPPh_2)]$ (8)

Heating a toluene solution (50 cm^3) of **8** (30 mg, 0.04 mmol) at reflux for 2 days resulted in a loss of the orange colour and formation of a black precipitate. IR and ^{31}P NMR spectra showed complete decomposition and chromatography produced no bands.

Reaction of $[Fe_2(CO)_6(\mu\text{-}CH_2PPh_2)(\mu\text{-}PPh_2)]$ (2) with allene

A toluene solution (100 cm^3) of **2** (0.29 g, 0.44 mmol) was cooled in a silica Young's tube (*c.* 200 cm^3) to −196 °C and evacuated, then allene (0.65 g, 17 mmol) was condensed in. The tube was slowly warmed to room temperature and placed under UV irradiation for 2.5 h, resulting in a colour change from yellow to red. Chromatography on Florisil in the dark gave a yellow band which eluted with diethyl ether–hexane (1:4) and afforded 90 mg of **2**. A dark red band eluted with diethyl ether–hexane (1:1) provided 148 mg (50%) of $[Fe_2(CO)_5\{\mu\text{-}\eta^1,\eta^3\text{-}PPh_2C(CH_2)_2\}(\mu\text{-}CH_2PPh_2)]$ (**10**), which afforded large dark red crystals from diethyl ether–pentane.

Protonation of $[Fe_2(CO)_5\{\mu\text{-}\eta^1,\eta^3\text{-}PPh_2C(CH_2)_2\}(\mu\text{-}CH_2PPh_2)]$ (10) in the presence of CO

Dropwise addition of 0.3 cm^3 of $HBF_4\cdot OEt_2$ (1.6 mmol) to a dichloromethane solution (70 cm^3) of complex **10** (80 mg, 0.12 mmol) while gently purging with CO produced a darkening of the solution. After 1 h, evaporation of the solvent and washing with several portions (3 × 20 cm^3) of diethyl ether gave a quantitative yield of $[Fe_2(CO)_7\{PPh_2C(Me)CH_2\}(\mu\text{-}CH_2PPh_2)][BF_4]$ (**11**) as a red powder.

Structure determinations of 3 and 5·Et_2O

Many of the details of the structure analyses carried out on **3** and **5**·Et_2O are listed in Table 5. X-ray diffraction measurements were made using Nicolet four-circle P3m diffractometers on single crystals mounted in thin-walled glass capillaries. Cell dimensions for each analysis were determined from the setting angle values of 23 and 20 centred reflections, respectively.

Intensity data were collected for unique portions of reciprocal space and corrected for Lorentz, polarisation and absorption effects, the latter on the basis of azimuthal. The structures were solved by heavy atom (Patterson and difference Fourier) methods, and refined by least-squares against *F*. All non-hydrogen atoms were assigned anisotropic displacement parameters. Methylene group hydrogen atoms were assigned refined isotropic displacement parameters and refined without positional constraints (except for H(1a) and H(1b) of **5**·Et_2O which were constrained to ideal geometries with C–H = 0.96 Å). All other hydrogen atoms were constrained to ideal geometries with C–H = 0.96 Å and assigned fixed isotropic displacement parameters (except the phenyl hydrogens in **5**·Et_2O for which displacement

TABLE 6. Atomic coordinates (×10^4) and isotropic thermal parameters (Å^2×10^3) for **3**

	x	*y*	*z*	*U*[a]
Fe(1)	788(1)	−1544(1)	2323(1)	44(1)*
Fe(2)	2890(1)	−1107(1)	2889(1)	44(1)*
P(1)	1201(1)	−2500(1)	1443(1)	38(1)*
P(2)	3120(1)	−1410(1)	1604(1)	39(1)*
O(2)	−1293(2)	−2248(2)	1891(2)	89(1)*
O(3)	107(2)	−111(1)	1056(1)	72(1)*
O(4)	2040(2)	675(1)	2360(2)	79(1)*
O(5)	4920(2)	−387(2)	3834(2)	97(1)*
O(6)	3501(2)	−2888(1)	3611(1)	64(1)*
O(10)	2866(2)	−726(2)	4633(1)	98(1)*
C(1)	2005(2)	−1992(2)	859(2)	41(1)*
C(2)	−479(2)	−1980(2)	2063(2)	59(1)*
C(3)	425(2)	−679(2)	1545(2)	51(1)*
C(4)	2319(2)	−35(2)	2539(2)	56(1)*
C(5)	4126(2)	−670(2)	3445(2)	62(1)*
C(6)	3218(2)	−2219(2)	3291(2)	48(1)*
C(10)	2425(2)	−988(2)	3911(2)	61(1)*
C(11)	1333(2)	−1298(2)	3649(2)	61(1)*
C(12)	1118(2)	−2214(2)	3554(2)	65(1)*
C(13)	542(2)	−680(2)	3287(2)	69(1)*
C(21)	1486(2)	−3998(2)	2488(2)	54(1)*
C(22)	1953(2)	−4780(2)	2863(2)	66(1)*
C(23)	2756(2)	−5122(2)	2644(2)	72(1)*
C(24)	3082(2)	−4703(2)	2032(2)	71(1)*
C(25)	2613(2)	−3922(2)	1638(2)	55(1)*
C(20)	1822(2)	−3552(2)	1875(1)	43(1)*
C(31)	−267(2)	−3721(2)	427(2)	61(1)*
C(32)	−1156(3)	−3948(2)	−236(2)	80(1)*
C(33)	−1688(2)	−3317(2)	−829(2)	74(1)*
C(34)	−1324(2)	−2464(2)	−761(2)	65(1)*
C(35)	−450(2)	−2228(2)	−90(2)	53(1)*
C(30)	88(2)	−2856(2)	517(1)	44(1)*
C(41)	4279(2)	−129(2)	1116(2)	76(1)*
C(42)	4440(3)	640(3)	705(3)	100(2)*
C(43)	3628(3)	1098(2)	174(2)	85(2)*
C(44)	2656(3)	806(2)	40(2)	72(1)*
C(45)	2484(2)	44(2)	446(2)	60(1)*
C(40)	3296(2)	−437(2)	986(1)	44(1)*
C(51)	4277(2)	−2395(2)	801(2)	55(1)*
C(52)	4905(2)	2092(2)	4239(2)	68(1)*
C(53)	4129(3)	1889(2)	3486(2)	77(1)*
C(54)	4173(2)	2178(3)	2703(2)	83(1)*
C(55)	5003(2)	2683(2)	2654(2)	63(1)*
C(50)	4211(2)	−2102(2)	1587(2)	45(1)*

[a]Starred items: equivalent isotropic *U* defined as one third of the trace of the orthogonalised U_{ij} tensor.

TABLE 7. Atomic coordinates ($\times 10^4$) and isotropic thermal parameters ($Å^2 \times 10^3$) for $5 \cdot Et_2O$

	x	y	z	U[a]
Fe(1)	9034(1)	1978(1)	3129(1)	38(1)*
Fe(2)	7131(1)	686(1)	2654(1)	36(1)*
P(1)	8084(2)	2752(2)	3778(1)	32(1)*
P(2)	6399(2)	1115(2)	3444(1)	31(1)*
O(2)	11016(5)	3050(6)	3549(3)	98(3)*
O(3)	9815(5)	−114(5)	3567(3)	67(3)*
O(4)	5202(5)	−441(5)	2207(3)	72(3)*
O(5)	8286(6)	−1375(5)	2804(3)	68(3)*
C(1)	6619(6)	2536(6)	3673(3)	32(3)*
C(2)	10219(7)	2628(8)	3389(4)	57(4)*
C(3)	9425(6)	677(7)	3396(3)	43(3)*
C(4)	5958(7)	9(7)	2392(3)	45(3)*
C(5)	7858(7)	−529(8)	2786(4)	49(4)*
C(11)	7660(2)	738(7)	1830(3)	57(4)*
C(12)	6675(5)	2139(8)	2237(3)	56(4)*
C(13)	7677(7)	1770(7)	2091(3)	45(3)*
C(14)	8701(7)	2262(7)	2297(3)	49(3)*
C(15)	8708(1)	3284(5)	2554(4)	59(4)*
C(16)	9688(5)	1691(3)	2358(4)	59(4)*
C(20)	8232(6)	4241(6)	3811(3)	37(3)*
C(21)	7569(7)	4963(7)	3507(4)	49(4)*
C(22)	7789(10)	6074(8)	3501(5)	70(5)*
C(23)	8666(10)	6478(9)	3804(4)	66(5)*
C(24)	9351(10)	5763(9)	4116(5)	71(5)*
C(25)	9121(7)	4664(8)	4116(4)	54(4)*
C(30)	8366(6)	2420(7)	4524(3)	37(3)*
C(31)	9131(7)	1662(7)	4696(3)	42(3)*
C(32)	9320(7)	1426(7)	5260(3)	52(4)*
C(33)	8752(7)	1937(8)	5654(4)	55(4)*
C(34)	7986(7)	2703(8)	5485(3)	52(4)*
C(35)	7790(7)	2946(7)	4926(3)	43(3)*
C(40)	4914(6)	997(6)	3377(3)	36(3)*
C(41)	4423(8)	31(7)	3480(3)	45(3)*
C(42)	3322(8)	−89(9)	3391(4)	52(4)*
C(43)	2689(7)	756(9)	3197(4)	64(4)*
C(44)	3168(8)	1733(10)	3094(4)	76(5)*
C(45)	4284(7)	1863(8)	3183(4)	54(4)*
C(50)	6682(6)	350(6)	4098(3)	35(3)*
C(51)	6224(7)	678(7)	4580(3)	48(3)*
C(52)	6452(8)	159(8)	5073(4)	58(4)*
C(53)	7128(8)	−734(9)	5100(4)	62(4)*
C(54)	7573(8)	−1084(8)	4630(4)	64(4)*
C(55)	7367(7)	−539(7)	4128(3)	50(4)*
O(60)	6005(11)	94(15)	623(4)	272(12)*
C(61)	7185(16)	−963(12)	432(7)	233(14)*
C(62)	6115(20)	−1212(20)	411(16)	476(35)*
C(63)	4989(11)	934(17)	777(5)	268(17)*
C(64)	4885(11)	2008(3)	640(6)	186(10)*

[a]Starred items: equivalent isotropic U defined as one third of the trace of the orthogonalised U_{ij} tensor.

parameters were allowed to refine freely). The solvent C–C and C–O distances were subjected to restraints.

The largest features of the final difference syntheses are close to the metal and solvent atoms. Refinements converged smoothly to residuals given in Table 5. Tables 6 and 7 report the positional parameters for these structure determinations. See also 'Supplementary material'. All calculations were made with programs of the SHELXTL-PLUS [38] system. Complex neutral-atom scattering factors were taken from ref. 39.

Supplementary material

Full tables of interatomic distances and bond angles, displacement parameters and observed and calculated structure amplitudes are available from the authors on request.

Acknowledgement

We are grateful to the SERC for the award of Research Studentships (M.L.T. and D.A.V.M.) and for support.

References

1 S.A.R. Knox, *J. Organomet. Chem., 400* (1990) 255.
2 F.A. Cotton and J.M. Troup, *J. Am. Chem. Soc., 96* (1974) 4422.
3 R.J. Puddephatt, *Chem. Soc. Rev., 12* (1983) 99.
4 E. Weiss and W. Hübel, *Chem. Ber., 95* (1962) 1179.
5 G. Hogarth, F. Kayser, S.A.R. Knox, D.A.V. Morton, A.G. Orpen and M.L. Turner, *J. Chem. Soc., Chem. Commun.,* (1988) 358.
6 N.M. Doherty, G. Hogarth, S.A.R. Knox, K.A. Macpherson, F. Melchior and A.G. Orpen, *J. Chem. Soc., Chem. Commun.,* (1986) 540.
7 G. Hogarth, S.A.R. Knox, B.R. Lloyd, K.A. Macpherson, D.A.V. Morton and A.G. Orpen, *J. Chem. Soc., Chem. Commun.,* (1988) 360.
8 N.J. Grist, G. Hogarth, S.A.R. Knox, B.R. Lloyd, D.A.V. Morton and A.G. Orpen, *J. Chem. Soc., Chem. Commun.,* (1988) 673.
9 P.E. Garrou, *Chem. Rev., 85* (1985) 171.
10 G. Hogarth and S.A.R. Knox, to be published.
11 H. Werner and R. Zolk, *Chem. Ber., 120* (1987) 1003.
12 B. Klingert, A.L. Rheingold and H. Werner, *Inorg. Chem., 27* (1988) 1354.
13 R. Regragui, P.H. Dixneuf, N.J. Taylor and A.J. Carty, *Organometallics, 3* (1984) 814.
14 L. Manojlovic-Muir, M.J. Mays, K.W. Muir and K.W. Woulfe, *J. Chem. Soc., Dalton Trans.,* (1992) 1531.
15 X.L.R. Fontaine, G.B. Jacobsen, B.L. Shaw and M. Thornton-Pett, *J. Chem. Soc., Dalton Trans.,* (1988) 1185.
16 R. Aumann and H.-J. Weidenhaupt, *Chem. Ber., 120* (1987) 23 and 105.
17 A.G. Orpen, L. Brammer, F.H. Allen, O. Kennard, D.G. Watson and R. Taylor, *J. Chem. Soc., Dalton Trans.,* (1989) S1.
18 A. Nakamura, *Bull. Chem. Soc. Jpn., 39* (1966) 543.
19 D.A.V. Morton and A.G. Orpen, *J. Chem. Soc., Dalton Trans.,* (1992) 641–653.
20 S. Otsuka, A. Nakamura and K. Tani, *J. Chem. Soc. A,* (1968) 2248.

21 J.A.S. Howell, J. Lewis, T.W. Matheson and D.R. Russell, *J. Organomet. Chem., 99* (1975) C55.

22 C.F. Putnik, J.J. Welter, G.D. Stucky, M.J. D'Aniello, Jr., B.A. Sosinsky, J.F. Kirner and E.L. Muetterties, *J. Am. Chem. Soc., 100* (1978) 4107.

23 R.P. Hughes and J. Powell, *J. Organomet. Chem., 54* (1973) 345.

24 M.R. Churchill and R. Mason, *Nature (London), 204* (1964) 777.

25 S. Aime, L. Milone and E. Sappa, *J. Chem. Soc., Dalton Trans.*, (1976) 838.

26 G. Conole, K.A. Hill, M. McPartlin, M.J. Mays and M.J. Morris, *J. Chem. Soc., Chem. Commun.*, (1989) 688.

27 D. Braga, A.J.M. Caffyn, M.C. Jennings, M.J. Mays, L. Manojlovic-Muir, P.R. Raithby, P. Sabatino and K.W. Woulffe, *J. Chem. Soc., Chem. Commun.*, (1989) 1401.

28 A.J. Deeming, A.J. Arce, Y. De Sanctis, P.A. Bates and M.B. Hursthouse, *J. Chem. Soc., Dalton Trans.*, (1987) 2935.

29 P. Bergamini, S. Sostero, O. Traverso, T.J. Kemp and P.G. Pringle, *J. Chem. Soc., Dalton Trans.*, (1989) 2017.

30 M.I. Bruce, O.B. Shawkataly and M.L. Williams, *J. Organomet. Chem., 287* (1985) 127.

31 P.S. Braterman, R.J. Cross and G.B. Young, *J. Chem. Soc., Chem. Commun.*, (1976) 1310.

32 S.O. Grim, R.P. Molenda and J.D. Mitchell, *J. Org. Chem., 45* (1980) 250.

33 A.D. Horton, A.C. Kemball and M.J. Mays, *J. Chem. Soc., Dalton Trans.*, (1988) 2953.

34 K.M. Henrick, M. McPartlin, J.A. Iggo, A.C. Kemball, M.J. Mays and P.R. Raithby, *J. Chem. Soc., Dalton Trans.*, (1987) 2669.

35 T.A. Albright, W.J. Freeman and E.E. Schweizer, *J. Org. Chem., 40* (1975) 3437.

36 F.A. Cotton and J.M. Troup, *J. Am. Chem. Soc., 96* (1974) 4155.

37 F.A. Cotton, B.E. Hanson, J.D. Jamerson and B.R. Stults, *J. Am. Chem. Soc., 99* (1977) 3293.

38 G.M. Sheldrick, *SHELTXL-PLUS,* Revision 2.4, University of Göttingen, Germany, 1988.

39 *International Tables for X-ray Crystallography,* Vol. IV, Kynoch, Birmingham, UK, 1974.